Modeling and Advanced Control Design for DC/DC Converters in Microgrids

Chris Leonard, Baylor Howard
Advisor: Dr. Jing Wang

May 9th, 2019

Abstract

Power grids are transforming into smarter ones with the increased integration of distributed renewable energy sources, such as solar and wind. Along with these advancements, microgrids are evolving and are going to dominate the future of energy distribution. In order to accomplish this, their development requires advanced sensors, controls and communications. In this project, we particularly study the advanced control strategy for DC/DC converters used in Microgrids. Modeling and control for both buck converter and boost converter are addressed, respectively. Specifically, after deriving the averaged state-space model for the converter, two control methods are proposed. The first one is simply based on linearization around the equilibrium point and a state feedback control is designed using the standard eigenvalue assignment method. However, the control input, which takes a signal from the duty cycle to the switching device, may be out of range with this design due to the nature of local approximation. To solve this problem, we propose the second solution, which is a new design based on nonlinear control method. We show this control algorithm can stabilize the system while ensuring the duty cycle is in the range of the system. Thorough simulations based on PSpice and Matlab/Simulink are conducted to validate the proposed advanced control methods.

Table of Contents

1. Introduction

Due to the continued usage of fossil fuels in order to reach increasing electricity needs, the environment is being damaged at an alarming rate. Renewable energy sources are a more environmentally friendly alternative as opposed to conventional energy sources, due to the minimal carbon footprint that is left behind; however as seen in Figure 1.1, the amount of renewable energy compared to other sources is small. Solar energy is one of these renewable sources, and one that in the near future will see a lot of growth due to it currently only accounting for an extremely small portion of all energy production as seen in Figure 1.1. The system that is being proposed is a photovoltaic (PV) micro-inverter which will be attached directly to a power grid. The advantage of a microgrid is that it allows for increased control of power distribution, reduction of power losses, and most importantly is the ability to operate without a connection to the main power grid.

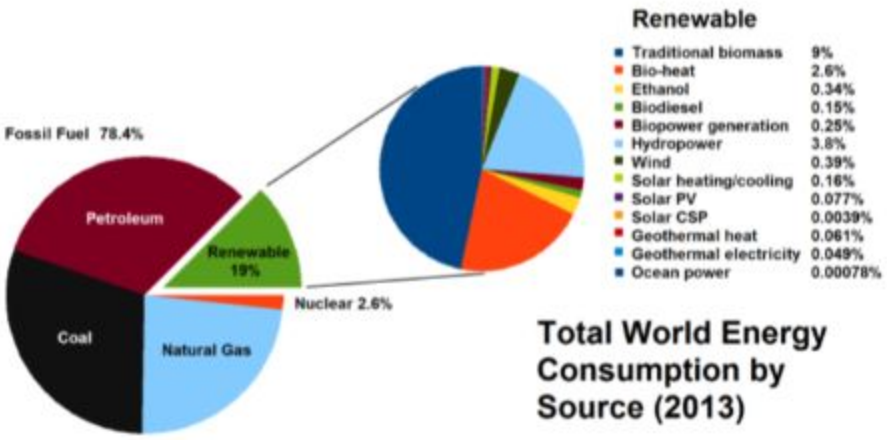

Figure 1.1: World Energy Consumption (2013) [1]

1.1 Project Background

The growth of renewable energy sources, namely within the photovoltaic sector, has been growing at an impressive rate within the past decade and this growth can continue with the development of more efficient and cost effective methods for energy production. Our project aims to improve power efficiency in microgrids by introducing the advanced control strategy for the DC/DC converters used in the system. This helps prevent power loss through the stabilization of the desired output in the presence of

disturbances. Better power efficiency makes implementing solar microgrids much more desirable than fossil fuel generator alternatives.

1.2 Problem Statement

The signal which will be received from the solar array is a DC signal, and in order for the power grid to be able to use this signal it is required to be inverted into AC power. The PV system can be broken into two subsystems which are the DC-DC converter and DC-AC inverter. The DC-DC converter which will be used in this system is to be a step-down buck converter in order to minimize losses and handle input perturbation. The design and implementation of both of these subsystems, as well as developing a signal tracking algorithm to ensure maximum power output are the problems this project will explore.

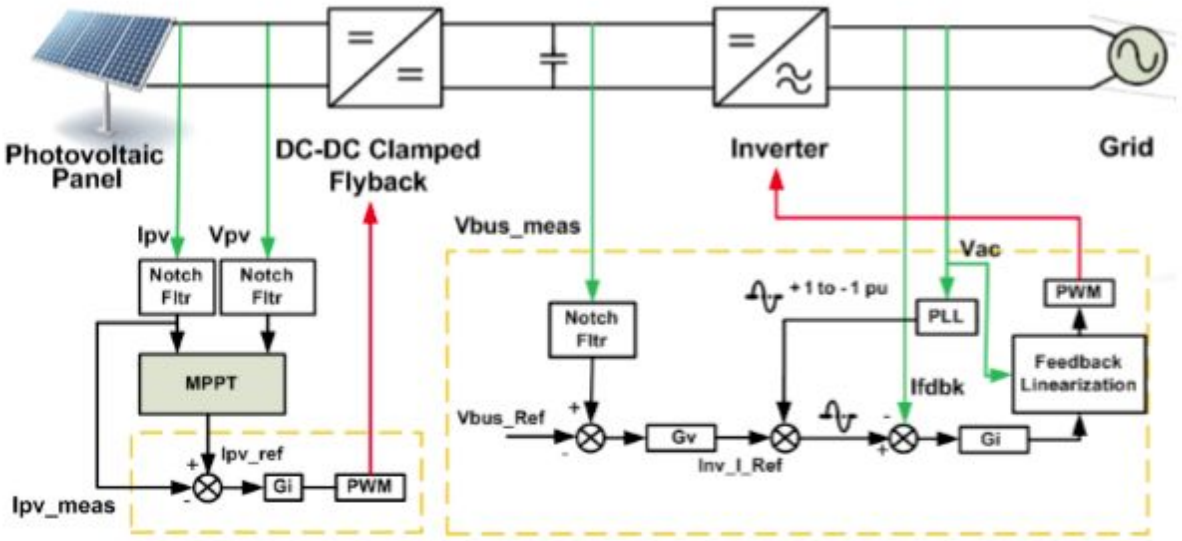

Figure 1.2: System Overview [1]

1.3 Objectives

The goal of this project is to successfully develop an advanced control algorithm for a DC-DC buck converter, and moreover to include both a linear and nonlinear model. The proposed model design must be non-model based as to not rely on system parameters. The PWM control signal must also be in range of the duty cycle. The system must be robust and thus be able to handle input perturbations as well as load uncertainty, as well as be able to handle existing ESRs from the inductors and capacitors.

2. Technical Approach and System Modeling

As previously stated, the system will be broken into two basic subsystems which are the DC/DC buck converter and the DC/AC inverter. A basic block diagram which outlines the construction of the microinverter can be seen in Figure 2.1. This system is able to take DC power which is provided by photovoltaic panels linked together in series and then convert the signal into a usable AC wave which is fed to a micro grid. The DC/DC converter is used to control the signal to a predetermined level as well as control the signal in the way of input voltage changes. The DC/AC inverter then is what allows the system to convert the signal into an AC signal which can be used by a grid.

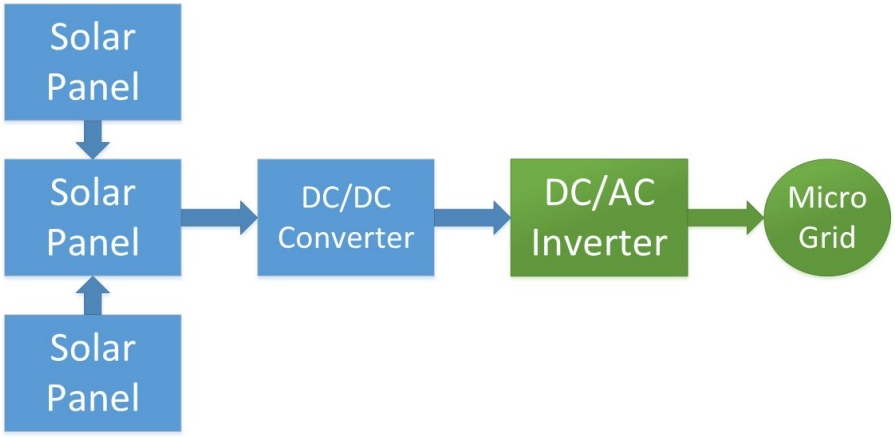

Figure 2.1: PV Microgrid Block Diagram

2.1. Subsystems

A DC/DC converter is to be used as the first subsystem within our design, which can be either a buck converter or a boost converter. A basic buck converter topology can be seen in Figure 2.2. Buck converters are used to step voltage levels down from one higher source level, to a lower output voltage. This voltage drop allows the buck converter to power electronics which otherwise would be overloaded by a high voltage input.

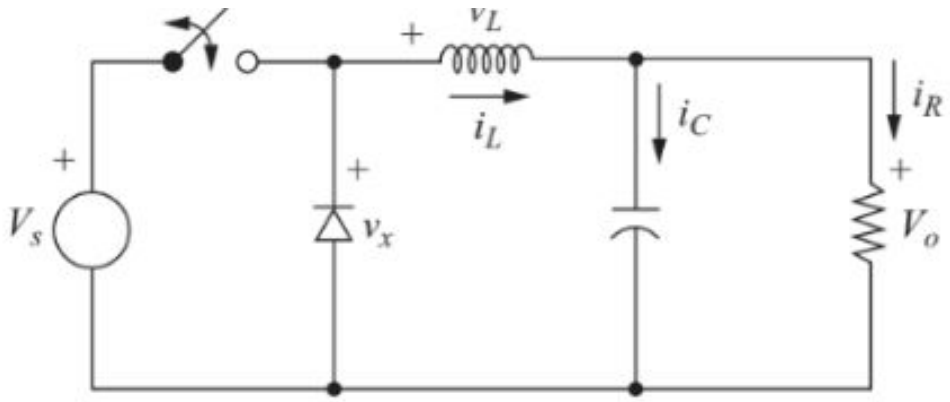

Figure 2.2: Buck Converter [3]

Boost converters can also be utilized within this system in lieu of a buck converter, and a simple boost converter topology can be seen in Figure 2.3. A boost converter is much like its buck counterpart, however instead of stepping voltage down, the boost converter can instead boost the signal from a low voltage level to a higher one. In addition to modifying the voltage level, the DC/DC converter subsystem will be used to track the maximum power point from the source signal, which allows the system to operate at maximum efficiency. The issue with boost converters however is that while the signal can be boosted to a higher level, this in turn boosts the errors and input changes within the signal itself. This is the main reason as to why we chose to instead use a buck converter within this system.

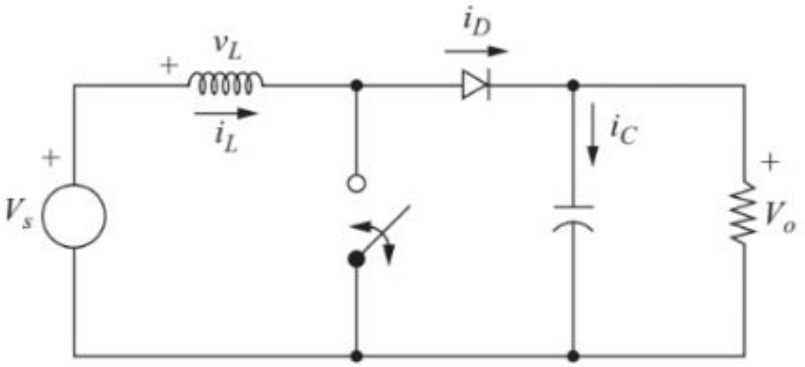

Figure 2.3: Boost Converter [4]

Aside from a DC/DC converter, an DC/AC inverter also is required, and a basic topology for this subsystem can be seen in Figure 2.4. The aim of the DC/AC inverter is to take the modified DC signal and convert it into a signal which can be effectively used by the power grid which the system will be connected to. The topology which is shown in

Figure 2.4 is known as an H-bridge inverter, and it is the most common and robust inverter type.

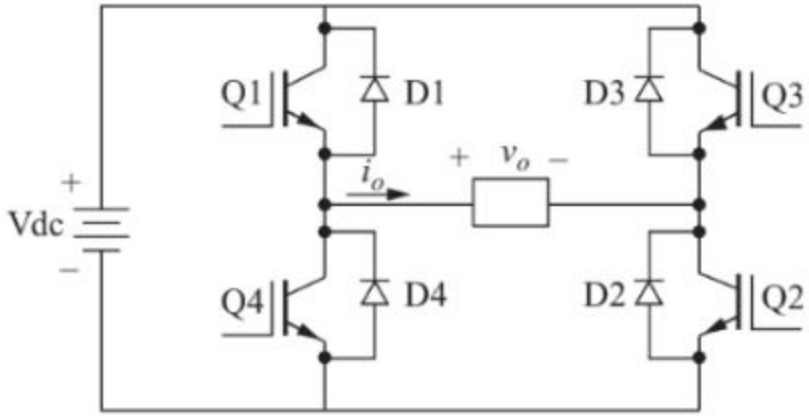

Figure 2.4: DC/AC Inverter [5]

2.2. Averaged State Space Model

In this section, we derive the state space model for the buck converter, which is used in the control design. A typical buck converter circuit is given in figure 1, in which there is a switch *S* (typically a MOSFET) that controls the circuit output. Let the switching frequency be $1/T_s$, where T_s is the period in secs. The switch opens and closes periodically within a switching period based on a duty cycle *D*, where $D \in [0,1]$. That is, for the kth switching peorid, $[kT_s, (k+1)T_s)$, the switch opens for the interval $[kT_s, (k+D)T_s)$, and closes for the interval $[(k+D)T_s, (k+1)T_s)$. The corresponding circuits are shown in figure 2 and figure 3, respectively.

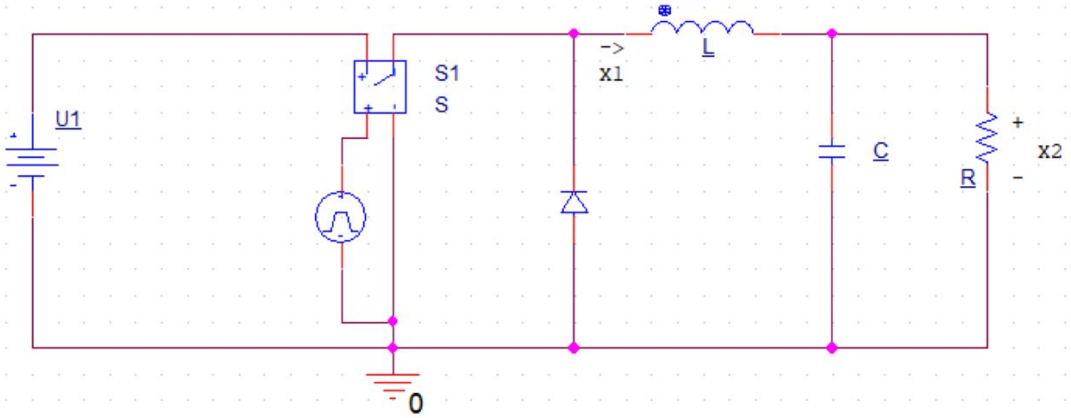

Figure 1: Buck Converter

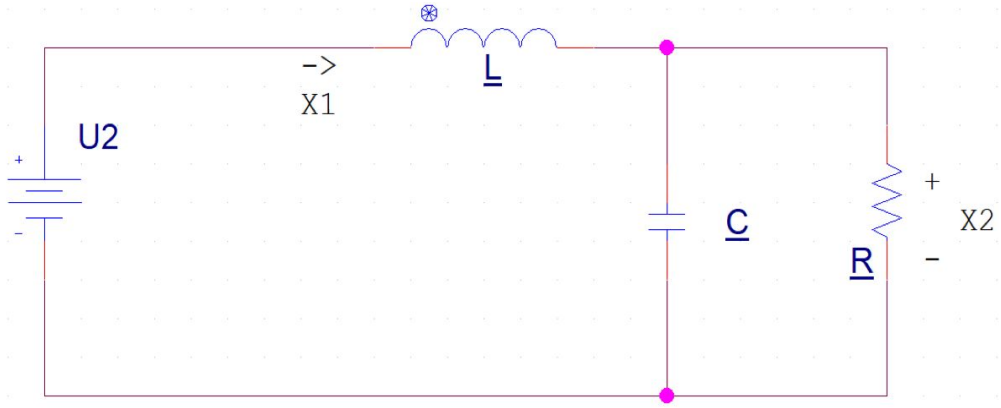

Figure 2: Buck converter with switching interval $[kT_s, (k+D)T_s]$

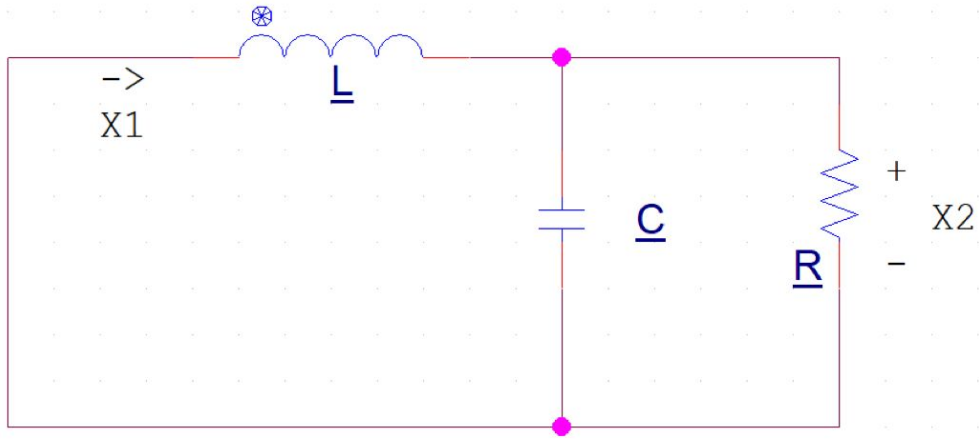

Figure 3: Buck converter with switching interval $[(k+D)T_s, (k+1)T_s]$

Assume that the buck converter is operating in a continuous-conducting mode, and the corresponding circuit model can be obtained using the basic circuit laws such as KVL and KCL. Define the state variables x_1 as the inductor current and x_2 as the capacitor voltage. For the switching interval $[kT_s, (k+D)T_s]$, we have

$$\dot{x} = A_1 x + B_1 V_s \tag{1}$$

where, $x = [x_1, x_2]^T$, V_s is the DC input voltage source, and

$$A_1 = \begin{bmatrix} 0 & -1/L \\ 1/C & -1/RC \end{bmatrix}, \qquad B_1 = \begin{bmatrix} 1/L \\ 0 \end{bmatrix}$$

For the switching interval $[(k+D)T_s, (k+1)T_s)$, we have

$$\dot{x} = A_2 x + B_2 V_s \tag{2}$$

with

$$A_2 = \begin{bmatrix} 0 & -1/L \\ 1/C & -1/RC \end{bmatrix}, \qquad B_2 = \begin{bmatrix} 0 \\ 0 \end{bmatrix}$$

To this end, the averaged state-space model for the circuit is

$$\dot{x} = Ax + BV_s \tag{2}$$

with

$$A = DA_1 + (1-D)A_2 = \begin{bmatrix} 0 & -1/L \\ 1/C & -1/RC \end{bmatrix},$$

$$B = DB_1 + (1-D)B_2 = \begin{bmatrix} D/L \\ 0 \end{bmatrix}$$

The averaged state-space model is an approximate one for studying the dynamical behavior of the buck converter. That is, under the assumption of ideal switcher, the input to the RLC circuit becomes a square wave. Based on the Fourier series of this square wave, it can be seen that the impact of harmonic terms is small when T_s is small enough or the circuit time constant is large enough. Its average DV_s dominates the circuit output, and this renders the averaged state-space model for ease of control design while without loss of practical accuracy.

The input signal which is fed to RLC circuits generally behaves like a square wave signal which has a frequency of $\frac{1}{T_s}$. If T_s is small enough, it is possible to use a Fourier analysis to show that the system output is dominated by the DC component of the square wave signal. By taking this into account, the average state space model which is used for the control design is $\dot{x} = Ax + BV_s$ where the values of A and B can be found below.

$$B = DB_1 + (1-D)B_2 = \begin{bmatrix} \frac{D}{L} \\ 0 \end{bmatrix} \quad A = DA_1 + (1-D)A_2 = \begin{bmatrix} 0 & -\frac{1}{L} \\ \frac{1}{C} & -\frac{1}{RC} \end{bmatrix}$$

3. Control Design

In this section, we present the proposed control designs for buck converter. The buck converter functions as a step-down DC/DC converter. Given the desired output capacitor voltage V_o^*, it follows from the averaged state-space model (3) that at the steady state

$$x_2^* = V_o^* = D * V_s,\ x_1^* = \frac{x_2^*}{R} = \frac{V_o^*}{R},\ D^* = \frac{V_o^*}{V_s}$$

3.1. Linear Design

Consider the averaged state-space model (3), the control could be done using the linear method based on its Jacobian linearization Define the error signal

$$e_1(t) = x_1 - x_1^*,\ \ e_2(t) = x_2 - x_2^*$$

It follows from (3) that the linearized model around the equilibrium point x_1^*, x_2^*, D^*, V_s is

$$\begin{aligned}\dot{e} &= \left.\frac{\partial f}{\partial x}\right|_{x_1^*,x_2^*,D^*,V_s} e + \left.\frac{\partial f}{\partial D}\right|_{x_1^*,x_2^*,D^*,V_s} \Delta D \\ &\quad + \left.\frac{\partial f}{\partial V_s}\right|_{x_1^*,x_2^*,D^*,V_s} \Delta V_s \\ &= Ae + \bar{B}\Delta D + \bar{B}_1 \Delta V_s\end{aligned}$$

where $f(x, D, V_s) = Ax + BV_s, \Delta D = D - D^*$, and ΔV_s representing the perturbation at the input source, and

$$\bar{B} = \begin{bmatrix}\frac{V_s}{L} \\ 0\end{bmatrix},\ \ \bar{B}_1 = \begin{bmatrix}\frac{D^*}{L} \\ 0\end{bmatrix}$$

The control design can be done based on pole-placement. Let the control be

$$\Delta D = -Ke \tag{4}$$

where K is selected such that the eigenvalues of the closed-loop system matrix $A - \bar{B}K$ are placed in the left half s-plane. That is, the characteristic equation given below

$$|sI - A + \bar{B}K| = 0$$

has all its roots in the LHP.

There are potential issues with the linear design. First, it is model based and if the circuit parameters change, then the control gain *K* may not be able to guarantee that the poles of $A = \overline{B}K$ are still in the LHP. Second, the value of ΔD in (4) may be out of range [0,1], and a scaling factor has to be introduced to produce the duty cycle in the range. However, this scaling factor would be depend on the value of ΔD and in general it has to be adjusted to make sure that $D + \Delta D$ are in the range of [0,1].

3.2. A New NonLinear Design

The proposed new control is based on the use of Lyapunov direct method. The proposed control is of the form

$$D(t) = D^* + \Delta D(t) = D^* - min\{D^*, 1 - D^*\}\frac{e_1}{1+e_1^2} \quad (5)$$

Under control (5), the stability of the closed-loop system can be shown as follows. Define the Lyapunov function candidate

$$V(t) = \frac{L}{2}e_1^2 + \frac{C}{2}e_2^2$$

Its time derivative is

$$\begin{aligned}
\dot{V}(t) &= Le_1\dot{e}_1 + Ce_2\dot{e}_2 \\
&= Le_1\left(-\frac{x_2}{L} + D(t)\frac{V_s}{L}\right) + Ce_2\left(\frac{x_1}{C} - \frac{x_2}{RC}\right) \\
&= Le_1\left(-\frac{x_2^* + e_2}{L} + D^*\frac{V_s}{L} + \Delta D\frac{V_s}{L}\right) \\
&\quad + Ce_2\left(\frac{x_1^* + e_1}{C} - \frac{x_2^* + e_2}{RC}\right) \\
&= \Delta D(t)V_s e_1 - \frac{e_2^2}{R} \\
&= -\min\{D^*, 1 - D^*\}\frac{V_s e_1^2}{1 + e_1^2} - \frac{e_2^2}{R} < 0
\end{aligned}$$

To this end, the stability of the closed-loop system follows.

It should be pointed out that $D(t)$ in (5) is in the range of [0,1]. And it does not rely on model parameters and is inherently robust to model uncertainties.

4. Simulation

Most of our research is done in PSpice and MATLAB simulation. We will briefly start by talking about the system parameters, followed by the linear DC/DC buck converter model, followed by the nonlinear DC/DC buck converter model.

4.1. System Parameters

Within the system the parameters which were used were an input voltage of 42V, however after 5ms this value then increased to 44V in order to show that the system was robust enough to handle changing input voltages. The system output which the buck converter stepped the signal down to is 12V, and by using both of these values which were chosen it is then possible to derive a duty cycle value. The duty cycle equation is $D = \frac{V_{out}}{V_{in}} = \frac{12}{42} = 0.286$ and this equation gives the system a duty cycle of 0.286. In addition to this, the resistive load which is used in the system is $R = 4\Omega$, the inductor is $L_1 = 1.33mH$, and the capacitor is $C_1 = 94\mu F$. This system is also using a PWM switching time of $T_s = 0.01ms$.

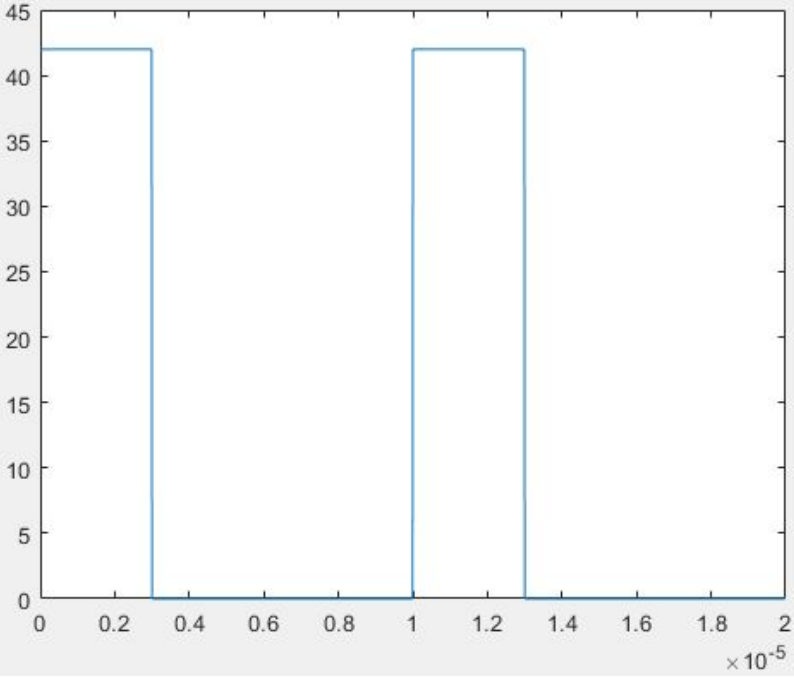

Figure 4.1 Matlab Generated Square Wave

This square wave generated in Matlab shows the voltage switching from 42V to 0V with a duty cycle of 0.286. As seen in Figure 4.1 the period starts at a voltage active high from 0 to 0.286 and then is at a voltage low of zero when the switch is off until the period ends. The sampling period shown above is 0.01ms. This figure demonstrates how the PWM switching is able to control the DC voltage and successfully step the voltage down to 12V.

4.2. Linear Model

The linear model for the buck converter can be seen in Figure 4.2. This linear model can easily be changed into a boost converter by changing orientation of the RLC components.

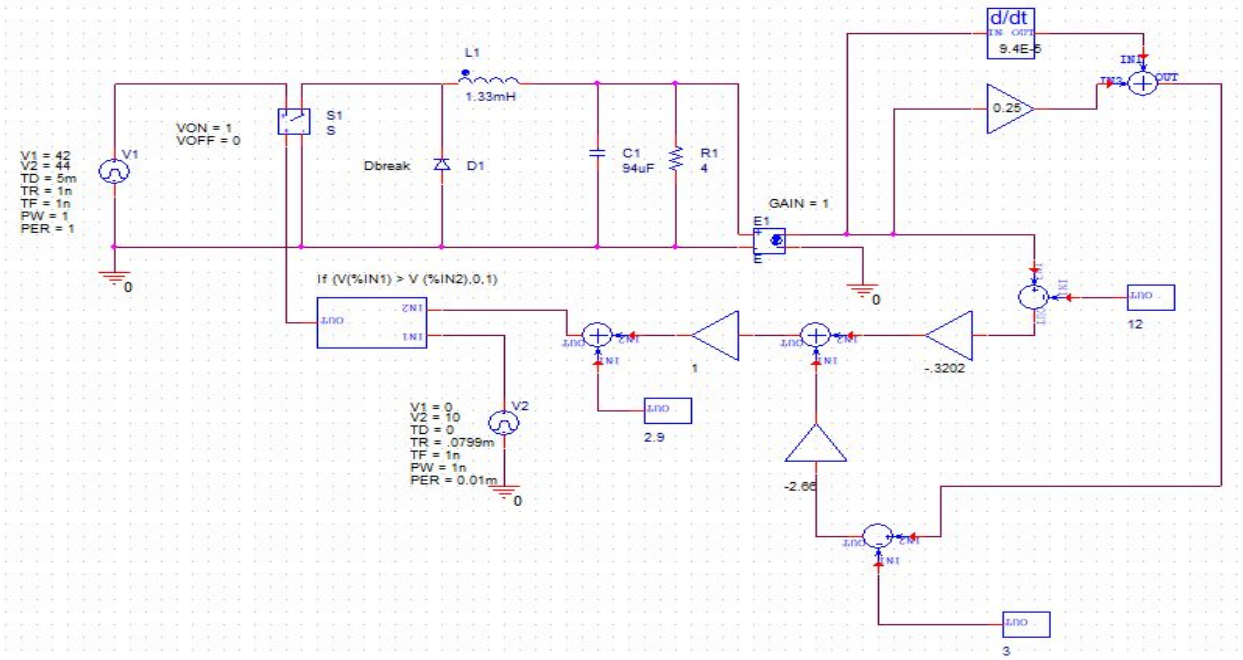

Figure 4.2 Linear Model of Buck Converter

In the Linear model, the input voltage is set to an arbitrary number, 42V, and is raised to 44V after 5 ms. This is done in order to test the robustness of input voltage change on the system. The Inductor component is 1.33mH, the Capacitor is 94μF, and the load resistor is 4Ω. The reference voltage that is being matched by the system is 12V. The duty cycle is calculated by using the equation: $D = \frac{V_{out}}{V_{in}}$ .Therefore the duty cycle on the switching component is set to 0.286. The switching on the sawtooth wave can be

set to a higher frequency to increase smooth signal reconstruction, however the buck converter becomes less efficient due to the power needed to drive the switch faster.

4.2.1 Linear Output

In Figure 4.3 below, the voltage output is shown in green from the DC/DC buck converter. The voltage hovers around 11.8V when the 42V signal is applied. When the signal switches over to 44V at 5ms, the voltage goes up to about 12.2V. These outputs are relatively close to the desired 12V. The advantage of the linear system is that it is a first order system that does not require the aid of a controller. To further smooth the output voltage, a simple averaging filter may be applied.

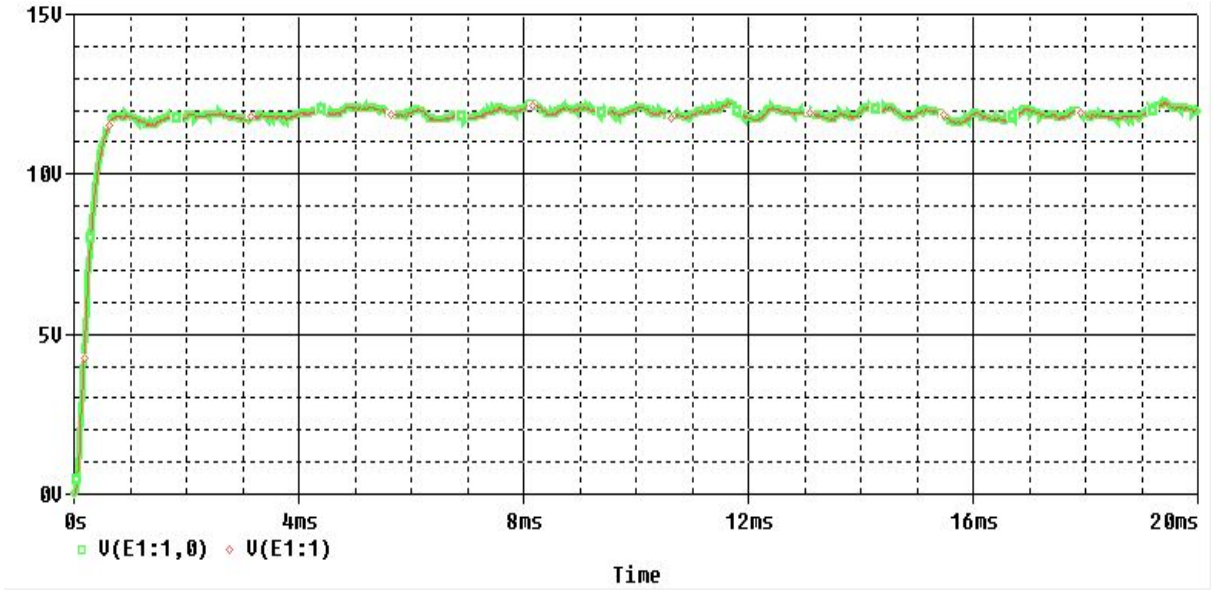

Figure 4.3 Linear Pspice Output -Transient sweep

4.2.2 Linear Monte Carlo

Testing the system model's ability to handle load change is done using a Monte Carlo Sweep. The component affected in this sweep is the load resistor. The resistor's properties are changed to 4Ω with a 5% tolerance. This tolerance demonstrates how a load change will affect the linear design shown in Figure 4.4

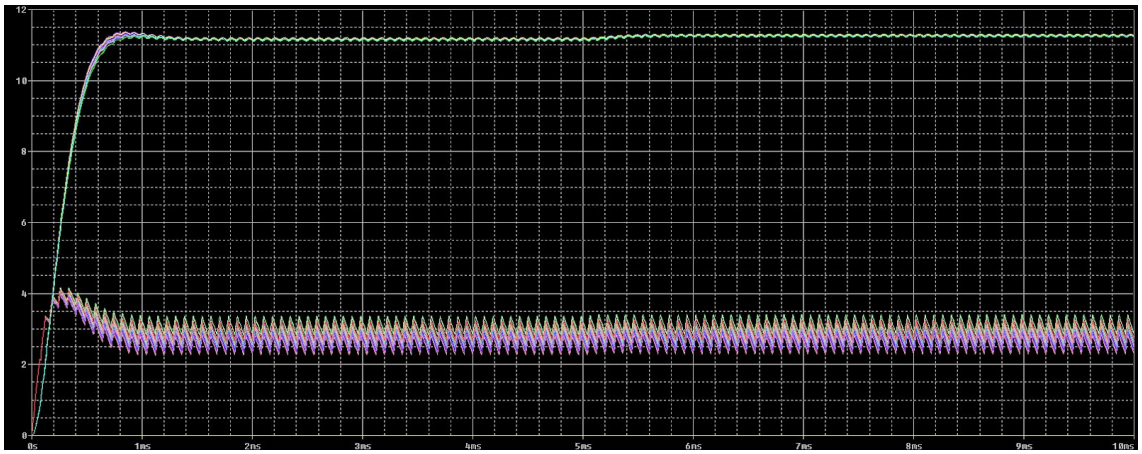

Figure 4.4 Linear Model PSpice Output - Load Monte Carlo

The Monte Carlo above shows little has changed for the green voltage output. However, the second smaller signal is the inductor current and it is not very stable under load change. The current varies from 3.4 to 2.4A. In order to correct this, a faster signal matching frequency is required than the one that is used in Figure 4.2.

4.2.3 Monte Carlo Histogram

A Histogram of the output voltage peaks are shown below in Figure 4.5. The number of samples used in this histogram is 50. We chose 50 because it was a large enough sample size to show the spread of signals without wasting simulation time. This histogram shows that the majority of the voltage in the linear model stays relatively close to 11.29V when the system experiences varying loads.

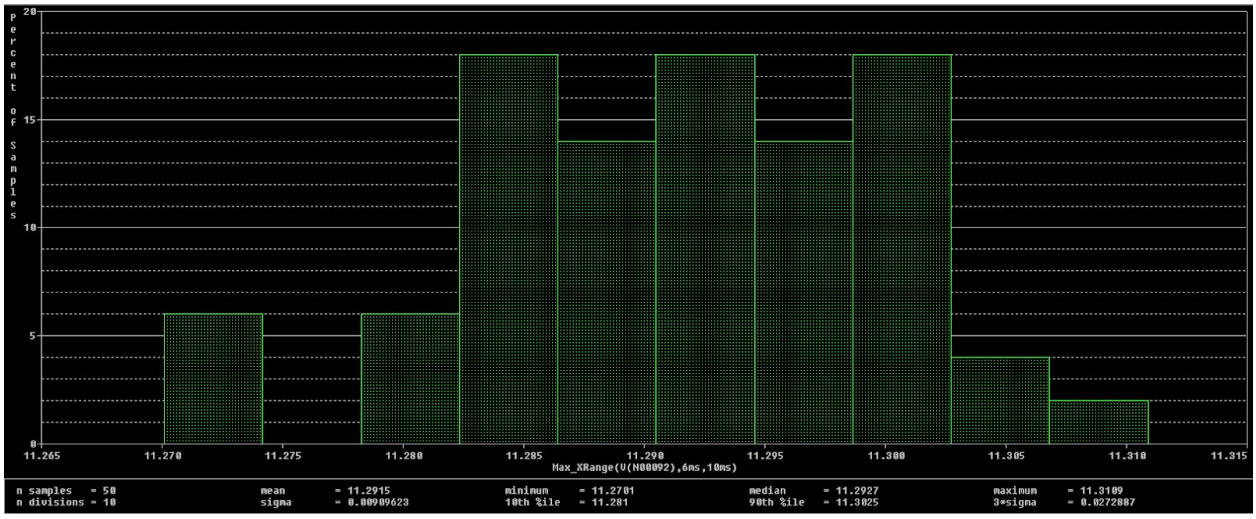

Figure 4.5 Monte Carlo Histogram

However, when simulating a Monte Carlo with the Inductor and Capacitor at 5% tolerance in combination with the load change, the linear model's voltage output was unstable and was unable to simulate in PSpice. This shows that for the linear system to work, all the component values need to be known otherwise the system may become unstable

4.3. NonLinear Model

The linear model for the buck converter can be seen below in Figure 4.2. This linear model can easily be changed into a boost converter by changing orientation of the RLC components. The nonlinear model is beneficial because the circuit itself is non-model based and requires no scaling factor or adjustment to be able to correctly buck to a determined voltage level.

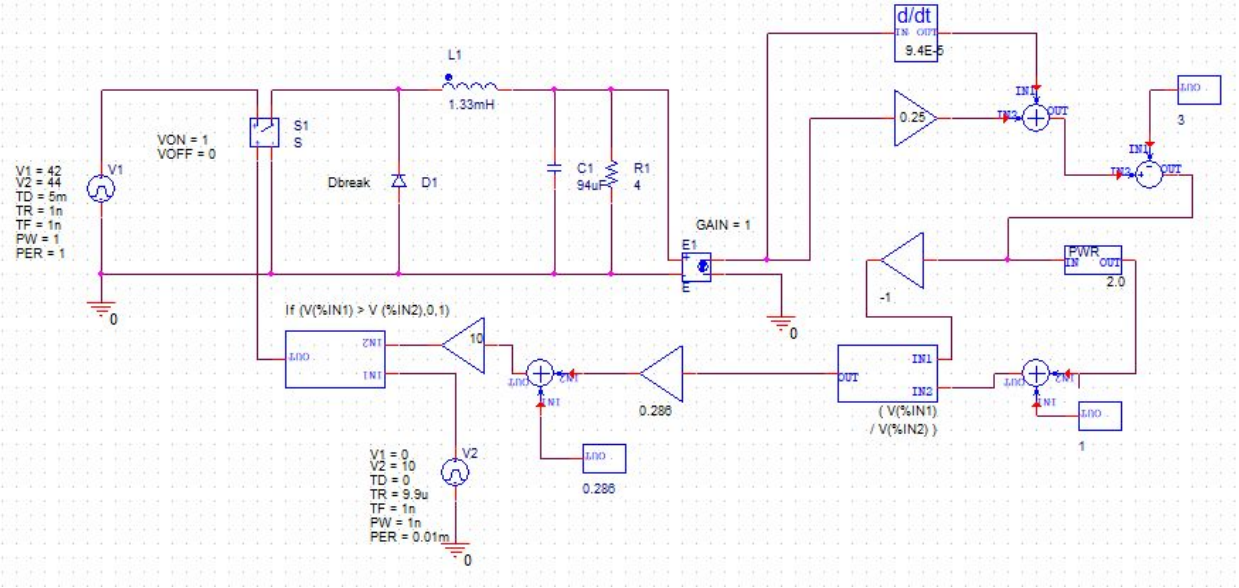

Figure 4.6 Nonlinear DC/DC Buck Converter Model

4.3.1 Nonlinear Output

The output plot for the nonlinear model can be seen in Figure 4.7. The red line denotes the output voltage signal which is being stepped down to roughly 12V, and the purple line shows the inductor current. This model allows us to use the inductor current value to obtain a better output, and an extremely small period is what allows the inductor current to look smooth as opposed to a sawtooth wave.

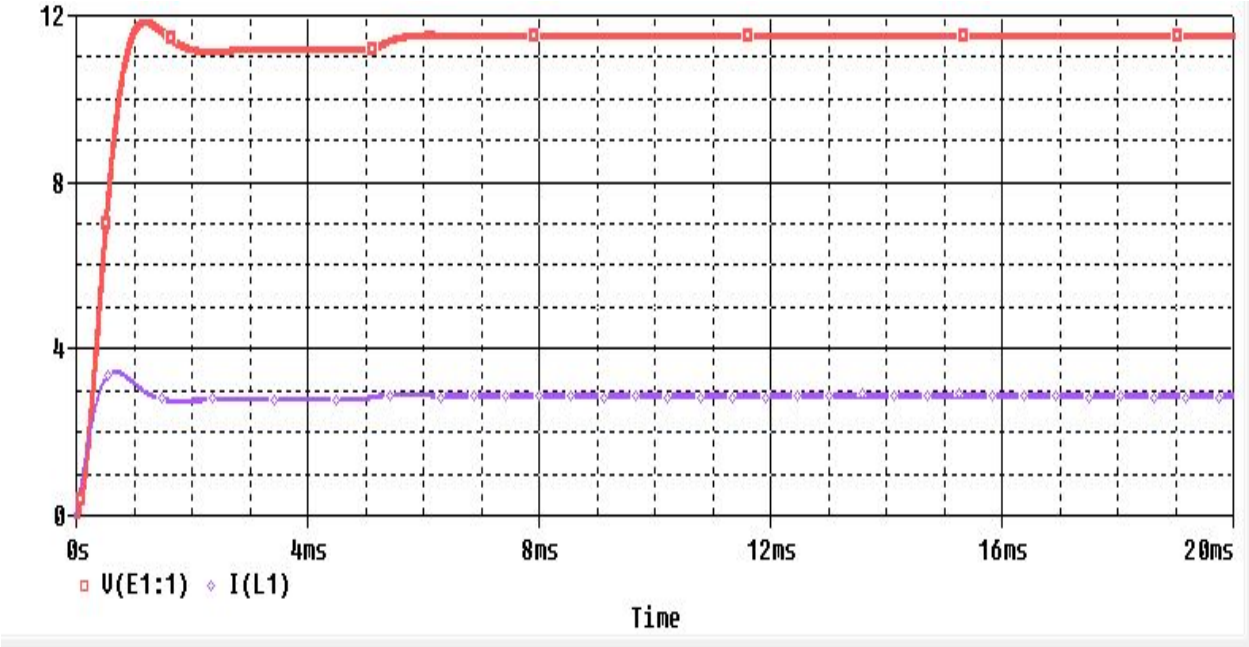

Figure 4.7 Nonlinear PSpice Output - Transient Sweep

4.3.2 Nonlinear Monte Carlo

In Figure 4.8 a monte carlo Pspice output can be seen which was run on the nonlinear system model. In this simulation a total of 50 iterations were used in order to obtain an adequate amount of outputs, and the resistive load was also allowed a 5% tolerance.

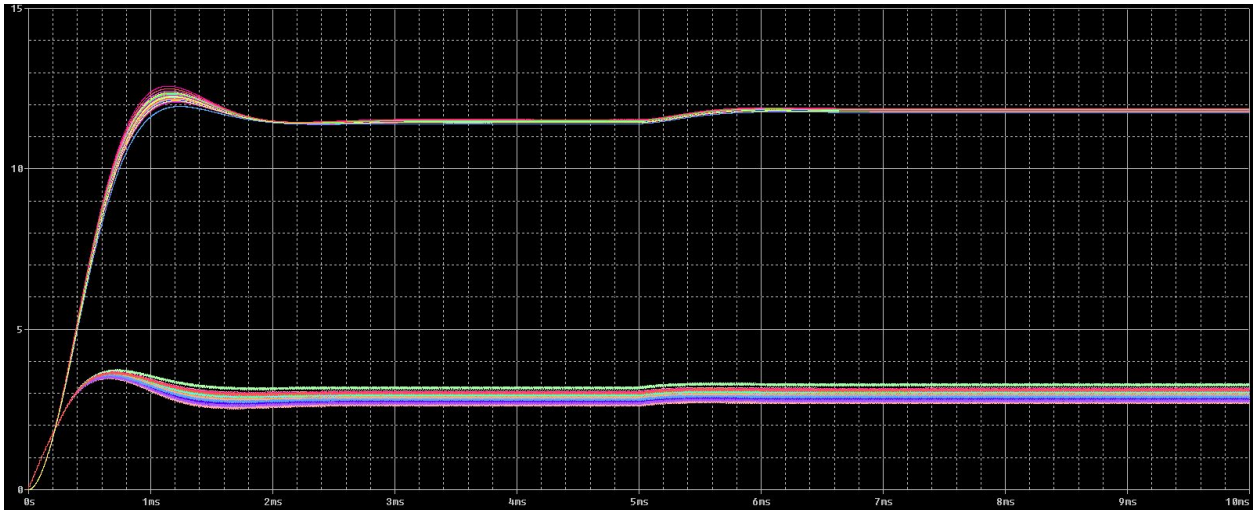

Figure 4.8 Nonlinear PSpice Output - Load Monte Carlo Load Variance

4.3.3 Monte Carlo Histogram

A Histogram of the output voltage peaks are shown below in Figure 4.9. Again, the number of samples used in this histogram is 50. We chose 50 to keep the sampling number consistent with the linear model's sample size. This histogram shows that the majority of the voltage in the linear model stays relatively close to 11.84V when the system experiences varying loads. This output is closer to the desired 12V than the linear model when put under varying load.

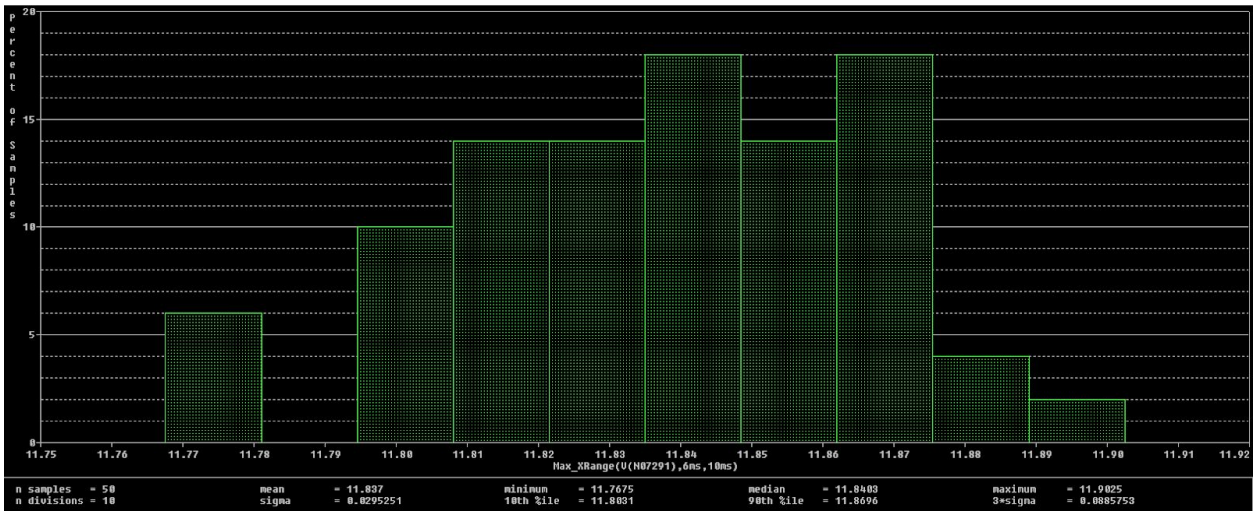

Figure 4.9 Nonlinear PSpice Output - Monte Carlo Histogram

4.3.4 RLC Monte Carlo

The next monte carlo test is with the inductor and capacitor tolerances at 5%. The nonlinear model is able to handle such tolerances and produced the spread of output signals below in Figure 4.10.

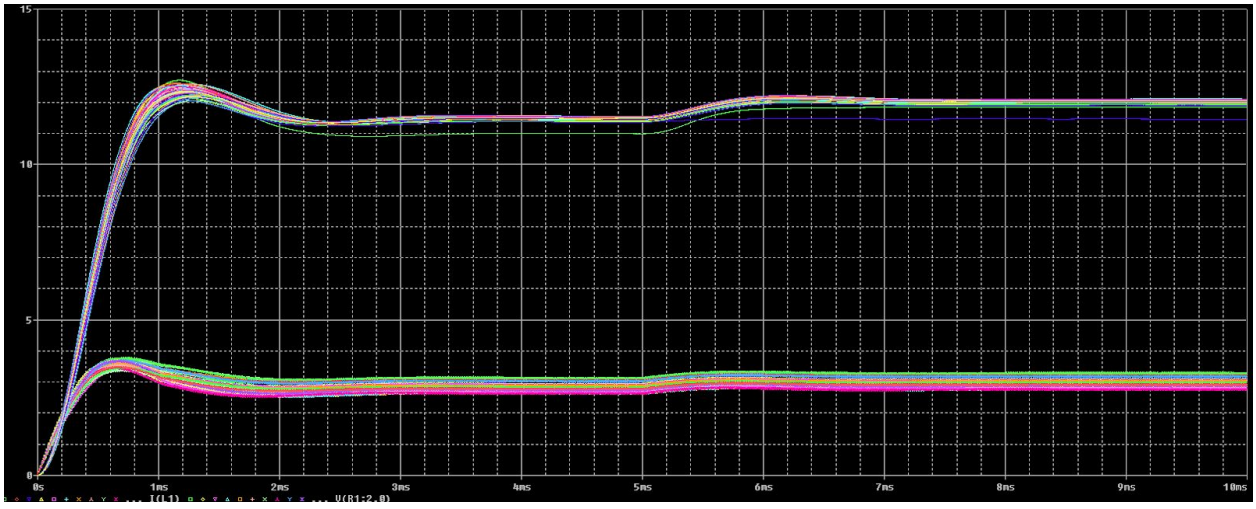

Figure 4.10 Nonlinear PSpice Output - RLC Monte Carlo

The larger signal is the output voltage over the varying load. Even though the components values are varying, the system's output voltage is relatively close to the desired output of 12V and the signal is smooth. The inductor current is also smooth even with the varying load and varying component values.

4.3.5 Monte Carlo Histogram

The monte carlo histogram shown below in Figure 4.11 is taken using 50 samples. We used 50 samples to keep consistency with the other histograms. The peak voltage output spread is shown below. Over 75% of the output voltage is directly on target with the desired output of 12V while the other 25% is within 0.2V of the desired output. This shows the robustness of the nonlinear model.

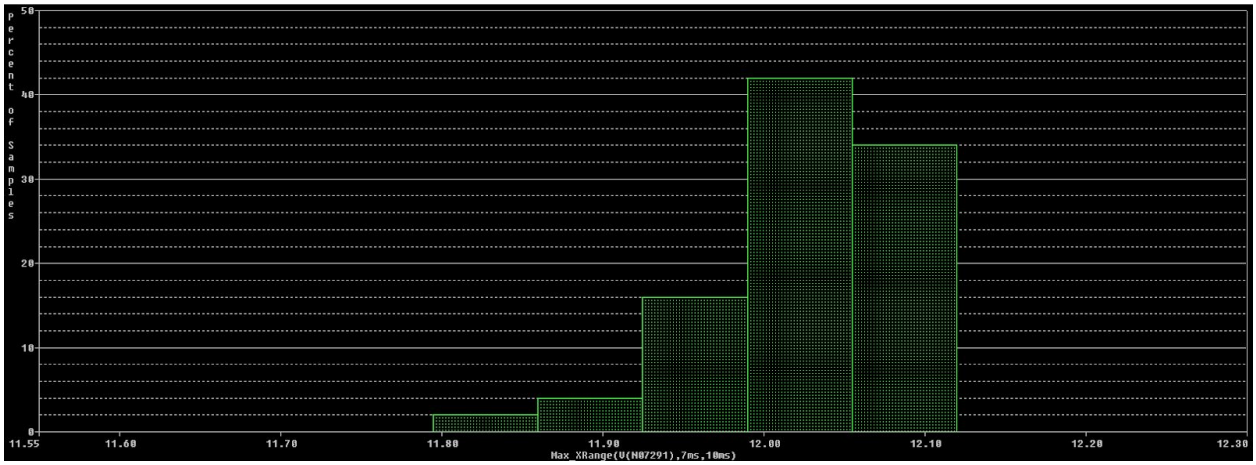

Figure 4.11 RLC Monte Carlo Histogram

5. Conclusion

Due to the environmental impact of finite fossil fuels on our atmosphere, it is imperative that we take the necessary steps towards sustainable energy sources such as solar power. Our system improves power efficiency in microgrids with its precise variable input tracking. This helps prevent power loss through tracking. Better power efficiency makes implementing solar microgrids much more desirable than fossil fuel generator alternatives.

6. Future work

While the DC/DC converter part of the overall system has been completed, in order to fully implement this system into a microgrid an inverter is needed. For this, development of an efficient H-bridge inverter is required, and after development of this component in completed it is then possible to use a C2000 micro inverter to fully implement the system.
When purchasing equipment, he buck converter as seen in Figure 6.1 cost about $200, the boost converter costs about $30, and the C2000 inverter cost $800. We will be using the DC power source in lab to simulate the solar panels, rather than using them so that we do not have to buy solar panels. Software such as MATLAB/Simulink and Pspice is also needed, however these tools are provided and common amongst the industry.

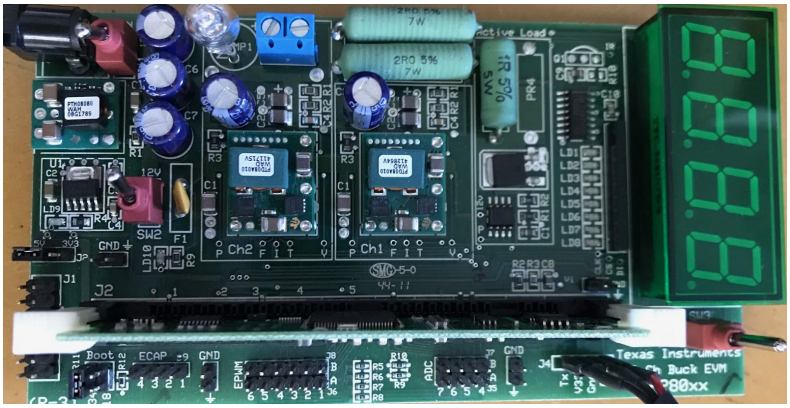

Figure 6.1: Buck Converter TMS320C2000

Other goals which can be explored in the future are attempting to expand the output in 3-phase AC power as opposed to the single phase which is currently planned. Means of energy storage would also be required to make the system work more efficiently in real world usage, and other work into expanding the efficiency of the photovoltaic panels which are used to generate the power.

7. References

1. Y. Lu, “Advanced grid-tied photovoltaic micro-inverter”, University of Canterbury, Christchurch, New Zealand, 2015.

2. Texas Instruments, “Digitally controlled solar micro inverter design using C2000 Piccolo microcontroller,” TIDU405B datasheet, Oct.2014 [Revised June 2017].
3. D. Hart, “Power Electronics.” New York: McGraw-Hill, 2011.
4. D. Hart, “Power Electronics.” New York: McGraw-Hill, 2011, p. 212.
5. D. Hart, “Power Electronics.” New York: McGraw-Hill, 2011, p. 337.
6. D. Hart, “Power Electronics.” New York: McGraw-Hill, 2011, p. 316.

APPENDIX A: Preliminary Converter Testing

Recreating the circuit shown in Figure 3.1 on page 316 in Daniel Hart’s *Power Electronics* [6], we were able to obtain an output voltage in similar fashion to the output voltage shown below in Figure 3.3. This confirms the circuit we built is close to how it is being used in the power electronics book. Once the output is consistent with input changes, we can continue moving forward with implementation onto a breadboard.

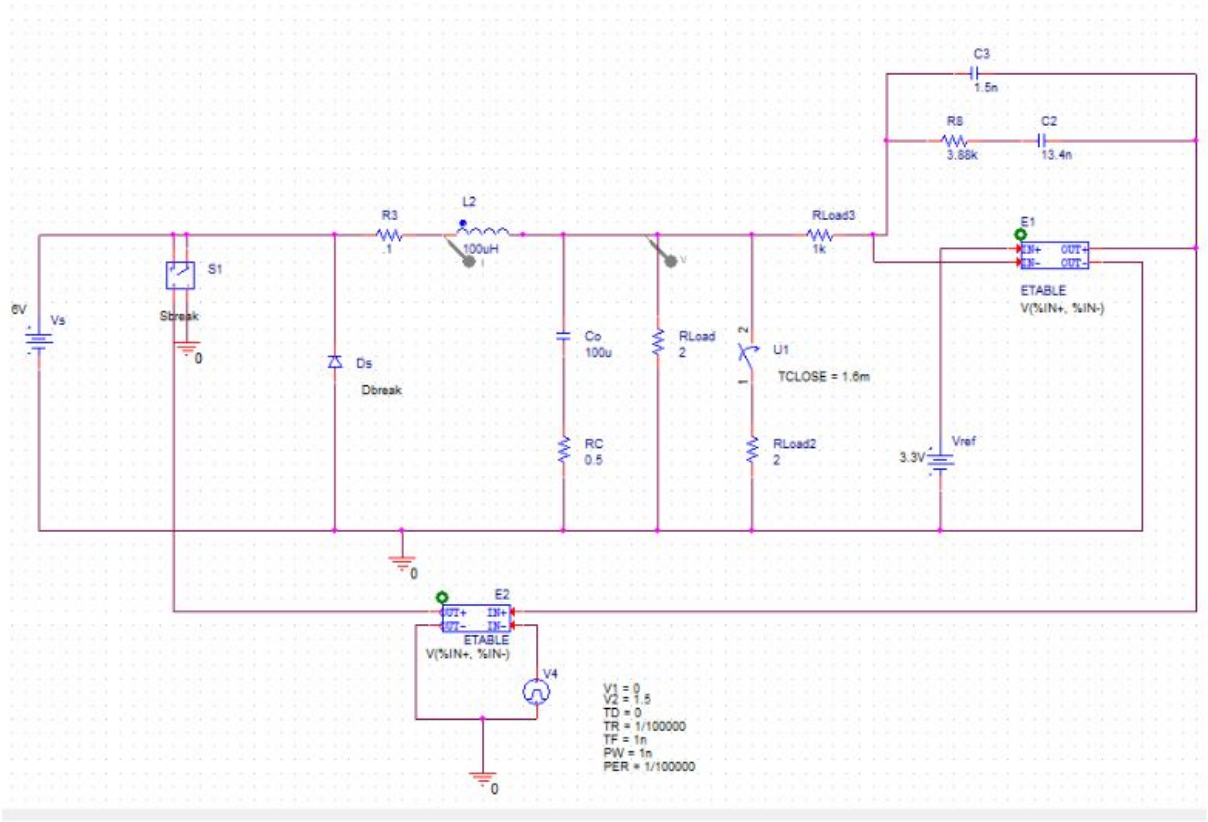

Figure 3.1: Buck Converter with Compensator in Pspice

In Figure 3.1, we are recreating the buck converter with compensator that is on page 316 of *Power Electronics.* Some of the parts were not in the general library but can be found in the following libraries:

- ETABLE parts can be found the ABM library folder.
- TCLOSE switch can be found in the Eval library folder.
- Sbreak S1 switch can be found in the Breakout library folder.

The Buck converter with compensator from the book did not behave how we initially believed it would. The output of the system gave us a voltage higher than the reference voltage which is not ideal. The output should be matching the input voltage to the lower reference voltage by recreating the signal using the sawtooth PWM generator located at the bottom side of the circuit. The purpose of the sawtooth signal is to compare the input with the reference voltage and recreate the reference signal, using the input signal.

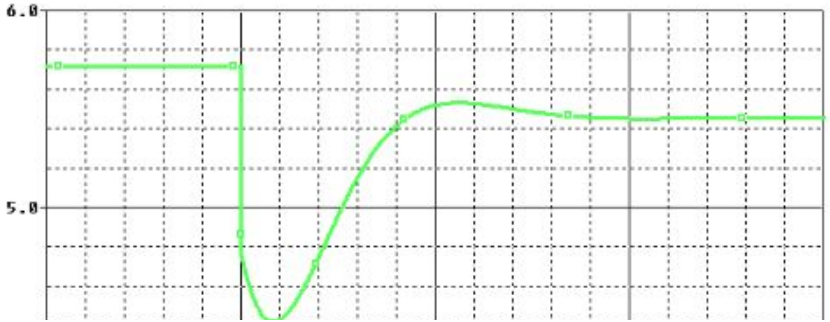

The load change shown in the figure above is shown when a switch is closed at 1.5ms after the circuit becomes active. The switch closing provides additional load to the circuit represented by the 2 ohm resistor the switch is connected to in Figure 2.2. The problem we encountered with the circuit shown on page 316 in *Power Electronics* is that the circuit does not track the reference voltage for the output. The goal of this circuit is to take a DC input and match its DC output to a reference voltage. The model is using an input voltage of 6 V and a reference voltage of 3.3 V. In Figure 3.2, the PSpice model does not have the output track the reference voltage because it is giving an output of approximately 4.8 V.

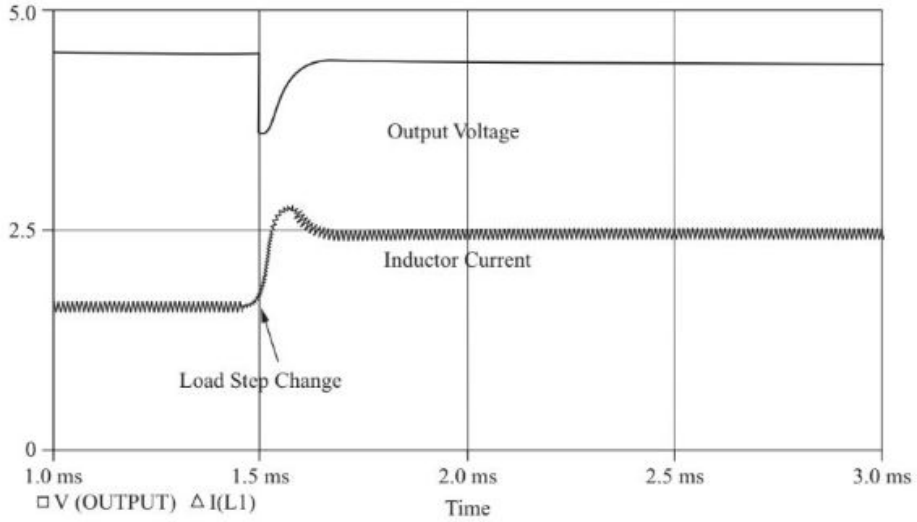

Figure 3.3: Expected Output Voltage [6]

We were unable to completely match the expected output in Figure 3.3, however minor modifications to the circuit will provide an output that is sufficient for our short term goal of becoming more familiar with buck converters. We are moving forward with our PSpice model by modifying the way the *Power Electronics'* circuit handles the reference voltage. Adding a buffer voltage to the input of the comparator should keep all the

values in the range of the saw tooth generated pwm. This will give the system a more robust way to track the input voltage.

APPENDIX B: Pspice Tutorial With ABM

In this tutorial of Pspice we are covering the general design and use of ABM blocks in the DC/DC buck converter. The following libraries are necessary to build our designs:

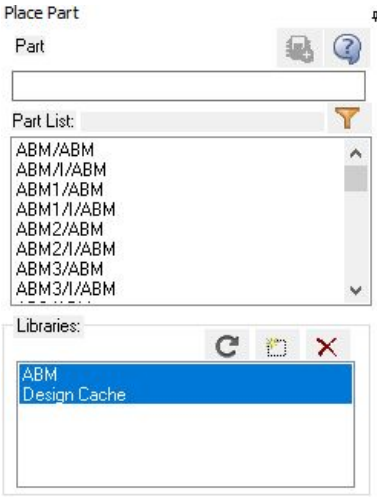

Figure B.1: ABM Library

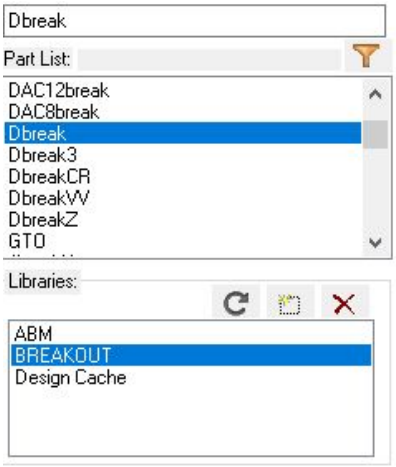

Figure B.2: DBreak Library

APPENDIX C: Matlab Code Simulation

In our matlab simulation, we show an inverter system. Shown below is the MATLAB code which was used to obtain the plot shown in Figure C.1.

```
% Dead beat control of inverter
% Feb 8, 2019
clc
clear all
Vp = 3; % peak value of AC voltage
f0 = 60; % reference sine wave frequency
f = 30*f0; % sampling frequency
T = 1/f; % sampling period
E = 5; % DC bus voltage
R = 2; %load resistance
L = 0.5*10^(-3); % filter inductance
C = 1000*10^(-6); % filter capacitance
t = 0:T:0.1;
number = length(t);
vc(1) =0.1;% output volatge
vcdot(1) = 0;% the derivative of output voltage
A = [0 1; -1/(L*C) -1/(R*C)];
B =[ 0; 1/(L*C)];

%Phi = exp(A*T);
Phi1 = [1-T^2/(2*L*C) T-T^2/(2*C*R); -T/(L*C) + T^2/(2*C^2*L*R) 1 - T/(C*R)+ (1/(C^2*R^2)-1/(L*C))*T^2/2];
```

```
Phi = [  0.6935        0.0004;
 -977.7458             0.4344];
for k=1:number

            vref(k) = Vp*sin(2*pi*f0*t(k));

            Error(k) = vref(k) - Phi(1,1)*vc(k) - Phi(1,2)*vcdot(k);%(1-T^2/(2*L*C))*vc(k) - (T-T^2/(2*C*R))*vcdot(k);

            Uinput(k) = sign(Error(k))*E;

            Delta_T(k) = Error(k)/(Uinput(k)*T/(L*C));

            %Gamma_Model = inv(A)*exp(A*((T-Delta_T(k))/2))*(exp(A*Delta_T(k))-[1 0; 0 1])*B;

            Gamma_Model = [Delta_T(k) Delta_T(k)*T; -T*Delta_T(k)/(L*C) -T*Delta_T(k)/(R*C)]*B;

            Vout =  Phi*[vc(k); vcdot(k)] + Gamma_Model*Uinput(k);

            vc(k+1) = Vout(1);

            vcdot(k+1) = Vout(2);

end
figure
plot(t, vc(1:number), t, vref(1:number));
xlabel('Time')
ylabel('Voltage')
```

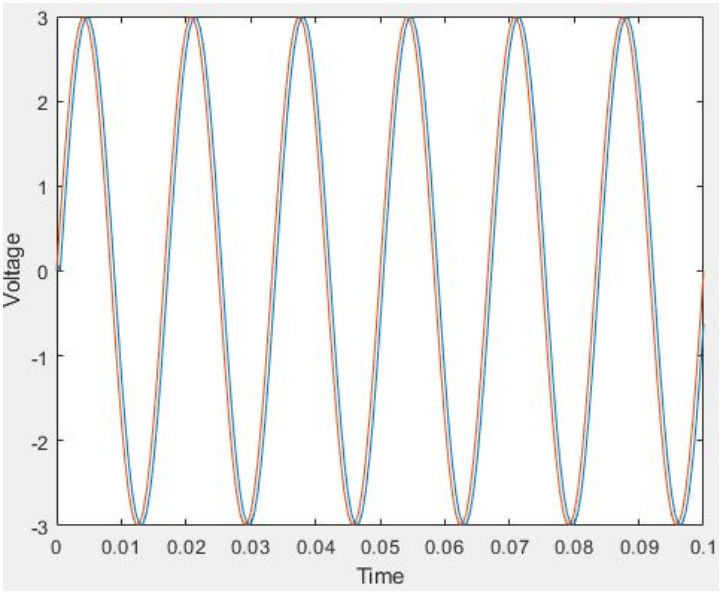

Figure C.1: Inverter Output from DC input

As seen in Figure C.1, the blue line is an AC signal of 6V peak to peak and the red line is the AC constructed signal.

APPENDIX D: Inverter Testing

Preliminary testing of an H-bridge inverter via the usage of Pspice can be seen in Figure D.1, and here an input voltage of 100V was used. With the system below it was then possible to obtain the output pictured in Figure D.2, which shows a peak to peak output voltage range of roughly 140V. This voltage range is from +70V to -70V, and these values were simply chosen at random for preliminary inverter testing purposes.

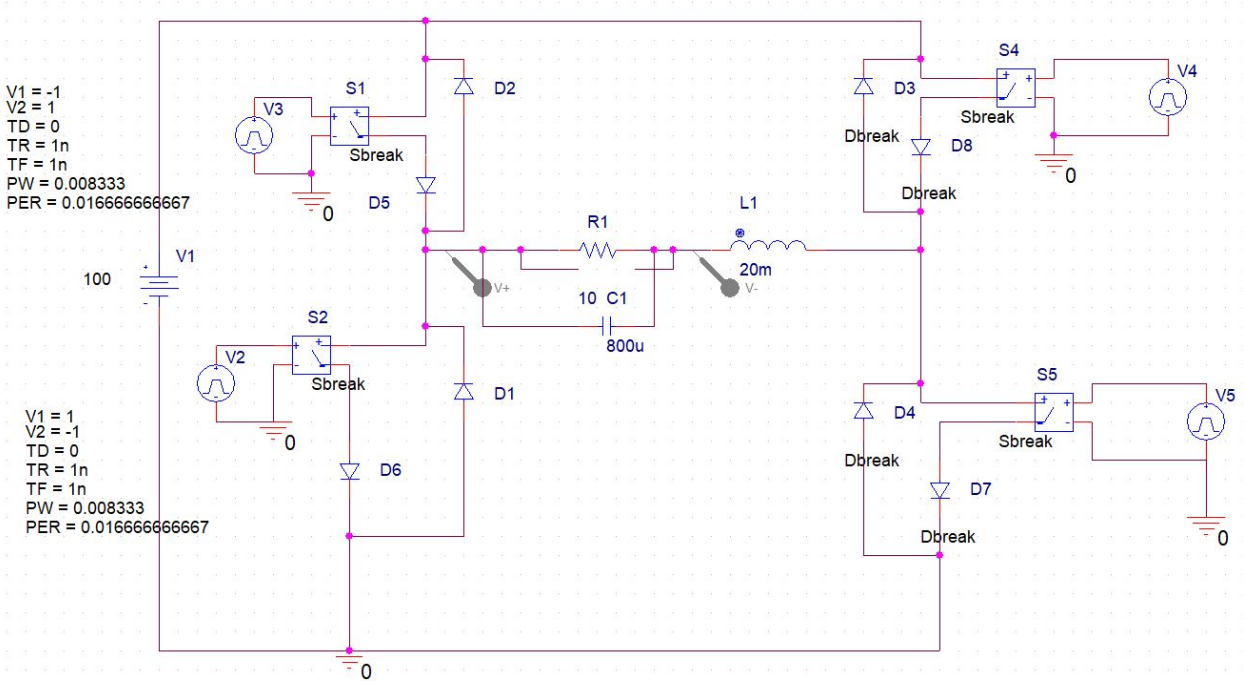

Figure D.1: DC/AC Inverter PSpice Model

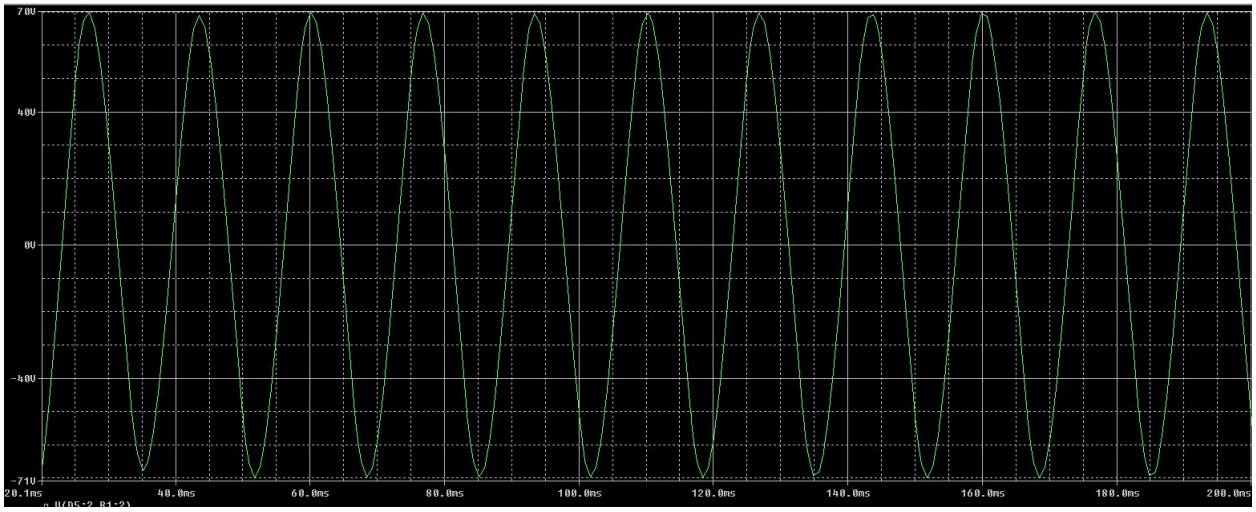

Figure D.2 DC/AC Inverter Output